# Accurate Potentials for Argon−Water and Methane−Water Interactions via ab Initio Methods and Their Application to Clathrate Hydrates

**Brian J. Anderson, Jefferson W. Tester, and Bernhardt L. Trout***

*Department of Chemical Engineering, Massachusetts Institute of Technology, 77 Massachusetts Avenue, 66-458 Cambridge, Massachusetts 02139*

*Received: June 13, 2004; In Final Form: September 20, 2004*

High level ab initio quantum mechanical calculations were used to determine the intermolecular potential energy surface between argon and water, corrected for many-body interactions, to predict monovariant and invariant phase equilibria for the argon hydrate and mixed methane−argon hydrate systems. A consistent set of reference parameters for the van der Waals and Platteeuw model, $\Delta\mu_w^0 = 1077 \pm 5$ kcal/mol and $\Delta H_w^0 = 1294 \pm 11$ kcal/mol, were developed for Structure II hydrates and are not dependent on any fitted parameters. Our previous methane−water ab initio energy surface has been recast onto a site−site potential model that predicts guest occupancy experiments with improved accuracy compared to previous studies. This methane−water potential is verified via ab initio many-body calculations and thus should be generally applicable to dense methane−water systems. New reference parameters, $\Delta\mu_w^0 = 1203 \pm 3$ kcal/mol and $\Delta H_w^0 = 1170 \pm 19$ kcal/mol, for structure I hydrates using the van der Waals and Platteeuw model were also determined. Equilibrium predictions with an average absolute deviation of 3.4% for the mixed hydrate of argon and methane were made. These accurate predictions of the mixed hydrate system provide an independent test of the accuracy of the intermolecular potentials. Finally, for the mixed argon−methane hydrate, conditions for structural changes from the structure I hydrate of methane to the structure II hydrate of argon were predicted and await experimental confirmation.

## Introduction

Water clathrates, often referred to as gas hydrates, are crystalline solids consisting of a three-dimensional host lattice of hydrogen-bonded water molecules arranged in such a way as to create cavities in which low molecular weight guest gas molecules are encaged. The two cavities of structure II hydrates are shown in Figure 1.

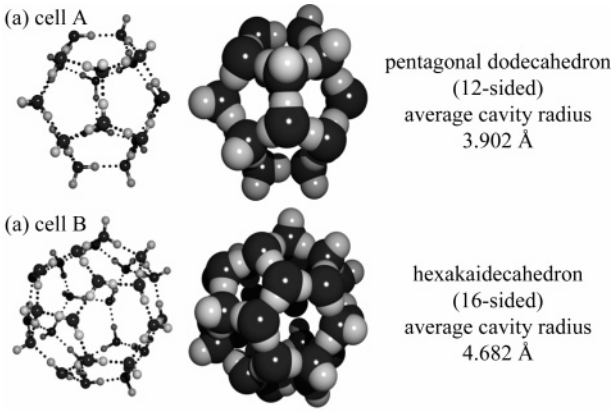


**Figure 1.** Cavities of structure II clathrates.

The structure II unit cell shown in Figure 2 has a lattice constant of 17.3 Å and consists of 136 water molecules that form 16 pentagonal dodecahedral cavities (cell A) and 8 hexakaidecahedral cavities (cell B). Thus for a completely occupied system, the ideal stoichiometry would be (16A,8B)·136 $H_2O$.

For decades, it was believed that small molecules, particularly those smaller than propane, formed only structure I clathrates. More recently, crystallographic measurements[1,2] have shown that Ar, Kr, $N_2$, and $O_2$ can form structure II clathrates. For the argon−water clathrate, both cells A and B can be occupied by argon molecules, so the fully occupied stoichiometry becomes $24Ar\cdot136H_2O$ or $Ar\cdot5\ ^2/_3H_2O$.

## Gas Hydrate Modeling

A thermodynamic model corresponding to the three-dimensional generalization of ideal localized adsorption was proposed in 1959 by van der Waals and Platteeuw.[3] By assuming single guest occupancy of the available water cages and negligible distortions of the empty lattice, the difference in chemical potential between the clathrate and empty host lattice can then be expressed as

$$\Delta\mu^{\beta-H} = kT\sum_i \upsilon_i \ln(1 + \sum_J C_{Ji}\hat{f}_J) \qquad (1)$$

where $\upsilon_i$ is the number of type $i$ cavities per water molecule, $\hat{f}_J$ is the fugacity of the guest molecule $J$, which is usually calculated from a mixture form of a PVTN Peng−Robinson equation of state,[4] and $C_{Ji}$ is the Langmuir constant for a guest molecule $J$ in a cavity of type $i$ defined as

$$C_{Ji} \equiv \frac{Z_{Ji}}{kT} = \frac{1}{8\pi^2 kT}\int_V \exp(-\Phi(r,\theta,\phi,\alpha,\beta,\gamma)/kT) r^2 \sin\theta\, dr\, d\theta\, d\phi\, d\alpha\, d\beta\, d\gamma \qquad (2)$$

* To whom all correspondence should be sent. E-mail: trout@mit.edu.

10.1021/jp047448x CCC: $27.50 
Published on Web 11/10/2004

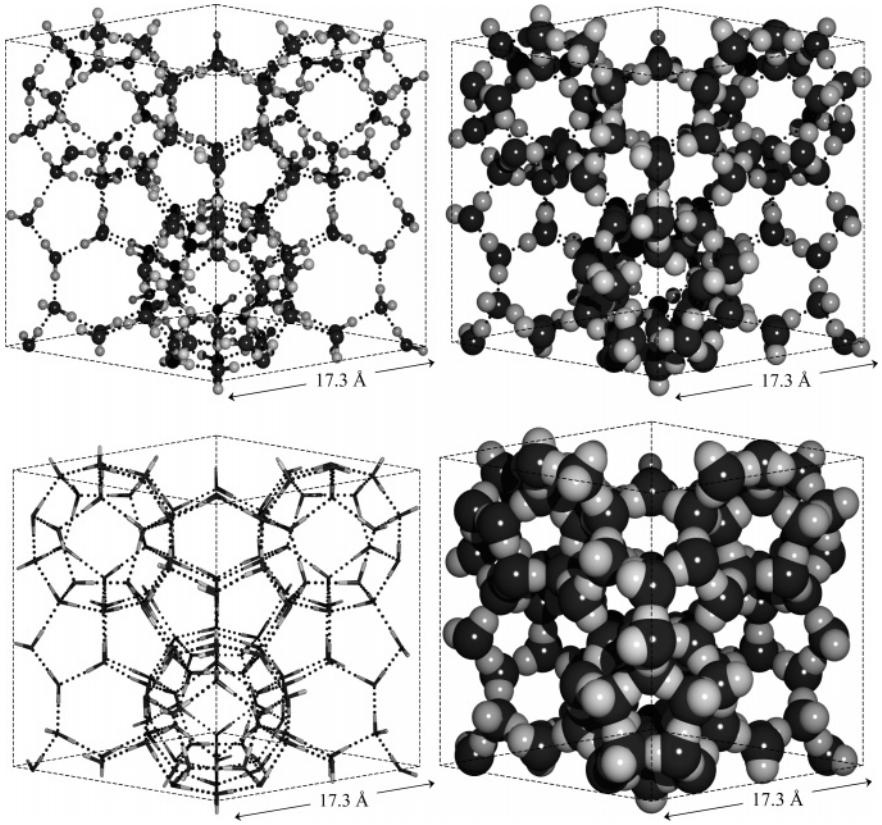


**Figure 2.** Ball and stick and space filling models of the structure II clathrate.

where $Z_{Ji}$ is the full configurational integral, which depends on the total interaction potential between guest and host molecules[5,6] and which is, in general, a function of $r$, $\theta$, and $\phi$, the polar coordinates of the guest molecule, and $\alpha$, $\beta$, and $\gamma$, the Euler angles that describe the orientation of the guest.

With this thermodynamic model, we can consider the clathrate as a two-component system, with monovariant, three-phase equilibrium described by

$$\mu_w^H = \mu_w^{L,\alpha}$$

$$\mu_w^\beta - \mu_w^H = \mu_w^\beta - \mu_w^{L,\alpha}$$

$$\Delta\mu_w^{\beta-H} = \Delta\mu_w^{\beta-L,\alpha} \tag{3}$$

where $\mu_w^\beta$ is the chemical potential of a hypothetical empty hydrate lattice, $\mu_w^H$ is the chemical potential of water in the hydrate phase, and $\mu_w^{L,\alpha}$ refers to the chemical potential of water in either a solid ice phase, $\alpha$, for $T \leq 273.15$ K or liquid aqueous phase, L, for $T \geq 273.15$ K. In the thermodynamic model, $\mu^{\beta-L,\alpha}$ can be determined from experimental data and $\hat{f}_J$ from a *PVTN* equation of state.

Following the convention proposed by Holder,[7] the chemical potential difference between water in the hypothetical empty lattice and the water in the hydrate phase can be expressed as

$$\frac{\Delta\mu_w^{\beta-L,\alpha}(T,P)}{kT} = \frac{\Delta\mu_w^{\beta-L,\alpha}(T_0,0)}{kT_0} - \int_{T_0}^{T}\left[\frac{\Delta H_w^{\beta-L,\alpha}}{kT^2}\right]_P dT + \int_0^P \left[\frac{\Delta V_w^{\beta-L,\alpha}}{kT}\right]_T dP - \ln a_w^L \tag{4}$$

where $\Delta\mu_w^{\beta-L,\alpha}(T_0,0)$ is the reference chemical potential difference at the reference temperature, $T_0$, and zero pressure. The temperature dependence of the enthalpy difference is given by

$$\Delta H_w^{\beta-L,\alpha} = \Delta H_w^{\beta-L,\alpha}(T_0) + \int_{T_0}^{T}\Delta C_p^{\beta-L,\alpha}\, dT \tag{5}$$

where the heat capacity difference is approximated by

$$\Delta C_{p_w}^{\beta-L,\alpha} = \Delta C_{p_w}^{\beta-L,\alpha}(T_0) + b^{\beta-L,\alpha}(T - T_0) \tag{6}$$

where $b^{\beta-L,\alpha}$ is the constant representing the dependence of heat capacity on the temperature. The volume difference, $\Delta V_w^{\beta-L,\alpha}$, is assumed to be independent of pressure. The additional term involving the activity of water, $a_w^L$, is defined by

$$a_w^L = \frac{\hat{f}_w^L}{\hat{f}_w^+} \tag{7}$$

where $\hat{f}_w^L$ is the fugacity of water in the water-rich aqueous phase and $\hat{f}_w^+$ is the water fugacity in the reference state, which is chosen to be the pure water phase at $T$ and $P$ of the mixture, thus using the conventional notation $\hat{f}_w^+ = f_w$. The reference temperature, $T_0$, is usually taken to be 273.15 K. Reference parameters reported in the literature are given in Table 1.

Having the ability to model accurately clathrate behavior, specifically phase equilibrium behavior, has been important in practical engineering operations. In 1939 Hammerschmidt[9] discovered that gas hydrates were forming plugs in natural gas transmission lines. This fact led to many investigations aimed at understanding and avoiding hydrate formation. Since the late 1950s, most modeling efforts have been based on the van der Waals and Platteeuw statistical mechanical model using the Lennard-Jones and Devonshire (LJD) spherical cell potential

**TABLE 1: Thermodynamic Reference Properties for Structure I and II Water Clathrates[8]**

| structure I (J/mol) | | structure II (J/mol) | | |
|---|---|---|---|---|
| $\Delta\mu^{\beta-L,\alpha}(T_0,0)$ | $\Delta H^{\beta-L,\alpha}(T_0,0)$ | $\Delta\mu^{\beta-L,\alpha}(T_0,0)$ | $\Delta H^{\beta-L,\alpha}(T_0,0)$ | source[a] |
| 699 | 0 | 820 | 0 | van der Waals and Platteeuw (1959) |
| | | 366−537 | | Barrer and Ruzicka (1962) |
| | | 833 | | Sortland and Robinson (1964) |
| 1255.2 | 753 | 795 | 837 | Child (1964) |
| 1264 | 1150 | | 808 | Parrish and Prausnitz (1972) |
| 1155 | 381 | | 0 | Holder (1976) |
| 1297 | 1389 | 937 | 1025 | Dharmawardhana, Parrish and Sloan (1980) |
| 1299 | 1861 | | | Holder, Malekar, and Sloan (1984) |
| 1120 | 931 | 1714 | 1400 | John, Papadopoulos, and Holder (1985) |
| 1297 | | | | Davidson, Handa, and Ripmeester (1986) |
| 1287 | 931 | 1068 | 764 | Handa and Tse (1986) |
| 1236 | 1703 | | | Cao, Tester, and Trout (2002) |
| 1203 | 1170 | 1077 | 1294 | this study |

[a] References 3, 11, and 21−30.

approximation.[3,10] Typically, phase data are fit by adjusting potential parameters for a specified pair potential model, commonly the Kihara potential. Evaluations at the University of Pittsburgh by Holder and co-workers[11] and at MIT[12] have demonstrated the inadequacy of the LJD approximation. These empirically fitted potential parameters are aphysical and cannot be applied to other systems such as mixed hydrate systems.[13] As one might expect, potential parameters computed from gas-hydrate phase data using the spherical LJD approximation do not match those computed from other experimental data.[8,11,14] Consequently, complete three-dimensional integration over the host lattice is necessary to determine correctly the full interaction energy.

In addition, recent work by Klauda and Sandler[15] showed that many-body interactions should be accounted for when applying computed potentials to the hydrate clathrate system. Proper determination of the form of the intermolecular interaction potential is also necessary both to compute equilibrium thermodynamic properties and to perform dynamic molecular simulations of kinetic phenomena such as diffusion and hydrate crystal nucleation, growth, and decomposition.

**Common Fit Potentials.** The ability to predict behavior in mixed systems, in which there is more than one type of guest molecule, is essential in predictions of naturally occurring hydrate systems. Commonly, the Lennard-Jones 6-12 or Kihara models are chosen to represent average interactions between the host water lattice and the guest molecules (methane, ethane, etc.) and are adjusted to fit experimental three-phase, monovariant dissociation pressure data as a function of *T*. Reference parameters are chosen a priori (Table 1) and the resulting fitted potential depends on the values of the reference parameters used. Thus, the potentials lack a physical basis, and must be determined ad hoc from data from each hydrate system studied. Furthermore, they cannot be consistently used where multiple clathrate cage types are occupied. Generating the potential surface from ab initio calculations becomes a promising alternative to these earlier empirical methods as interactions between guest and host molecules can be described in a molecularly consistent, quantitative manner.[16] For example, ab initio methods can be used to compute accurately the interaction energy of any particular orientation of the molecule pair. Suitable averages can then be obtained to functionally represent the spatial dependence of $\Phi_{ij}$ for all guest−host interactions needed to evaluate eq 2.

**Independently Determined Potentials.** Lennard-Jones parameters for liquid hydrocarbons have been optimized to reproduce experimental densities and heats of vaporization with an accuracy of approximately 5% in what is termed the OPLS model.[17] A popular model for water is the TIP3P model, which has three point charges on the oxygen and hydrogens to represent the dipole, and Lennard-Jones parameters for the oxygen only. The TIP3P model has been parametrized to reproduce liquid water properties at ambient conditions.[18] However, using a simple mixing rule, the TIP3P model and the OPLS model for hydrocarbons failed to give a reasonable Langmuir constant, a key term in the van der Waals and Platteeuw statistical model, for several hydrates.[6,12,19] In our previous work,[19,20] we use an intermolecular potential developed for methane clathrate-hydrates to capture, from first principles, accurate structure I methane clathrate reference parameters. This potential has been studied further in this work and modified according to the new methods employed for our new argon−water potential.

**Reference Parameters.** Accurate values for the thermodynamic reference parameters used in the van der Waals and Platteeuw statistical mechanical model are essential. The two critical reference parameters, $\Delta\mu_w^0$ and $\Delta H_w^0$, have been determined by many investigators.[3,11,21−30] Unfortunately, these parameters take on a wide range of values (see Table 1) and have so far been used in models to fit experimental data rather than to make predictions.[30]

## Objectives of This Work

To determine accurate, physically based, and model independent interaction parameters, we performed ab initio quantum mechanical calculations to determine guest−host interaction energies. First, we developed accurate intermolecular interaction potentials from ab initio calculations. Then an accurate and efficient method to calculate the potential energy surface was determined while considering the fineness of the intermolecular orientation grid as well as other factors, such as many-body effects, correlation dependencies, and basis set convergence. This accurate intermolecular potential is then used to determine with a low degree of uncertainty reference parameters for the van der Waals and Platteeuw model for hydrate clathrate systems. This model is then validated by predicting the cage occupancies for the methane hydrate system and then used to calculate pure argon hydrate phase behavior and predict the phase behavior of the argon−methane mixed hydrate system.

## Methodology and Approach

In our study, the aug-cc-pVQZ basis set was used for the calculation and the electron correlation energy was corrected by the second-order Møller−Plesset (MP2) perturbation method. Basis set superposition error (BSSE) was corrected by using

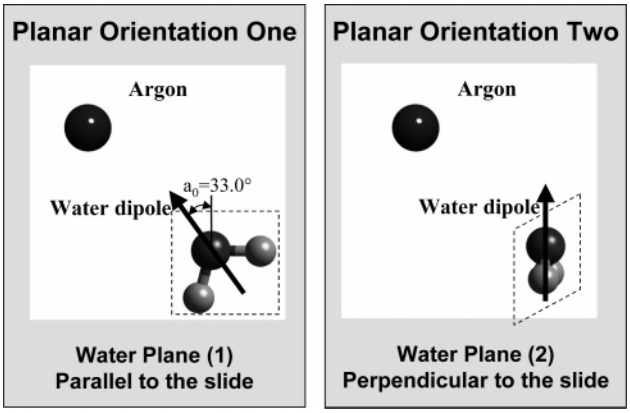


**Figure 3.** Two characteristic water plane orientations in the argon−water clathrate viewed from the center of the cavity.

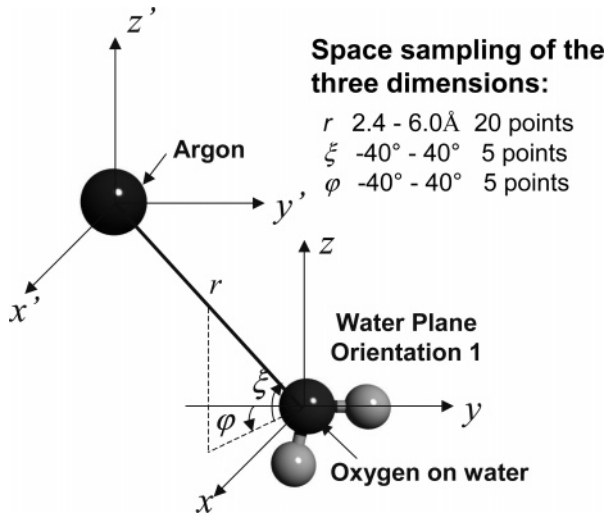


**Figure 4.** Three spherical coordinate dimensions ($r$, $\xi$, $\varphi$) used to define the position and orientation between an argon guest and fixed planar orientation 1 water host molecule.

half of the correction energy in the counterpoise method.[31] The geometry of the water molecules was optimized at the MP2/6-31++G(2d,2p) level. Gaussian 98 was used to perform the ab initio calculations.

**Determination of Potential Energy Surface.** In our calculation of interaction energies, the distance and orientation between argon and water are varied but the geometry of the water is frozen on the basis of the actual clathrate structure. By inspecting the ball-and-stick model of a structure II clathrate hydrate (see Figure 2), the relative orientations between guest and water molecule can be seen to fall into two types, characterized by the plane containing the water molecule, shown in Figure 3. The different orientations are then created by a two-step process: first fixing the planar orientation of the water molecule and then moving the guest molecule in the three-dimension grid to different positions inside the water cage. The center of mass of the guest molecule is moved in a polar coordinate system where the water oxygen is the origin. For guest molecules that are not spherically symmetric, such as methane, the rigid-body of the guest molecule is further rotated in its own internal coordinate in a fashion consistent with the geometry input file in the Z-matrix form, used in Gaussian 98 software (see ref 19). The combination of these two steps for the spherically symmetric guest argon maps out a simplified three-dimensional grid, as shown in Figure 4.

The range of the $r$, $\xi$, and $\phi$ dimensions given in Figure 4 were determined in the following manner. Because the guest molecule is entrapped in a single cage, the $r$ distance between the center of the argon guest and the oxygen atom of the host water molecule cannot be larger than the maximum diameter of the cage nor any smaller than the hard sphere radius of the Ar−O pair. Also, noting that the interaction energy will become extremely repulsive when the distance is very small, the interval for $r$ was set at 2.4−6.0 Å with 10 equally separated points selected. Ranges for the polar angle $\xi$ and azimuthal angle $\phi$ were determined by moving a guest molecule over a minimum distance inside the cage not too close to the cage wall. The $\xi$ and $\phi$ ranges were set from −40° to +40°. Five angular points were considered to be sufficient for sampling the argon−water configuration space.

For each separation distance $r$, there are two different water planes, and $5 \times 5 = 25$ angular orientations of the argon molecule. Therefore, an algorithm must be applied to combine the set of $25 \times 2 = 50$ interaction energies to obtain a potential that can be incorporated into the configurational integral. Two approaches were examined, an angle-averaging method that results in a potential dependent upon $r$ only, and a site−site method that attempts to account for guest orientation. In general, to determine the angle-averaged interaction, a Boltzmann-weighted average is taken at each radial point $r$ as a representative average of the five remaining degrees of freedom ($\alpha$, $\beta$, $\gamma$, $\xi$, and $\phi$) following the method outlined in Cao et al.[20] This angle-averaged potential, we found, results in large errors in the prediction of the occupancies of the clathrate cages. This error is due to the smearing effect of averaging out all of the five orientational and rotational degrees of freedom. The higher energy configurations are weighted out in the development of the two-dimensional potential but are calculated in the configurational integral.

To account for all six degrees of freedom in the argon− and methane−water interactions, a site−site model was developed. The 500 different argon−water and 18 000 different methane water orientations were fit to site−site potentials on the basis of the interactions between the center of the guest molecule and the oxygen on the water (**Ar**−**O**$H_2$ and $H_4$**C**−**O**$H_2$), the center of the guest molecule and the hydrogens on the water molecule (**Ar**−**H**OH and $H_4$**C**−**H**OH), and the methane hydrogens with the oxygen on the water ($H_3$C**H**−**O**$H_2$). The **Ar**−**O**$H_2$ and $H_4$**C**−**O**$H_2$ potentials capture the guest position effects whereas the **Ar**−**H**OH and $H_4$**C**−**H**OH potentials capture the $\xi$ and $\phi$ orientations. In addition, for methane, the $H_3$C**H**−**O**$H_2$ potential captures the Euler orientation of the methane molecule with respect to the water.

To obtain a highly accurate ab initio potential, we evaluated three energetic corrections: a correlation correction based on the effects of higher orders of quantum calculations, a basis-set extrapolation to ensure that the basis set employed can estimate interaction energies accurately, and a many-body correction to account for the many-body effects expected to play an important role in clathrate calculations. The effect of the level of correlation was examined by calculating a few selected points at increasing levels of electron correlation. It has been reported[32] that for hydrogen-bonded complexes, the improvements resulting from electron correlation beyond the MP2 level are not large. In this work, that improvement was investigated for the Ar−$H_2O$ pair. An ab initio potential was calculated for the Ar−$H_2O$ pair at the MP2 level using the 6-31++G(2*d*,2*p*), aug-cc-pVTZ, aug-cc-pVQZ, and aug-cc-pV5Z basis sets to examine the convergence of the potential with increasing basis-set size. As shown in Figure 5, the binding energy or the Ar−$H_2O$ complex converges (when using diffuse functions in the

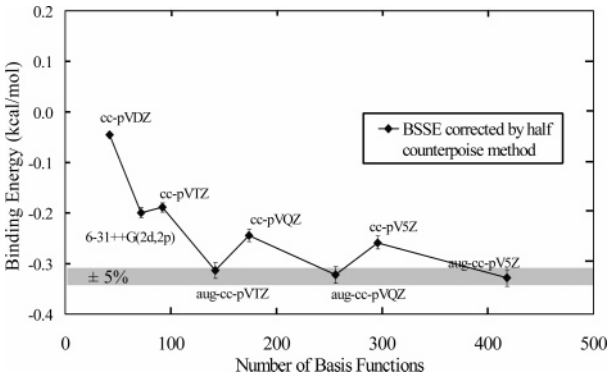


**Figure 5.** Effect of size of the basis set on estimated binding energy of the optimized Ar−$H_2O$ pair. ±5% deviation shown from aug-cc-pV5Z basis set calculation.

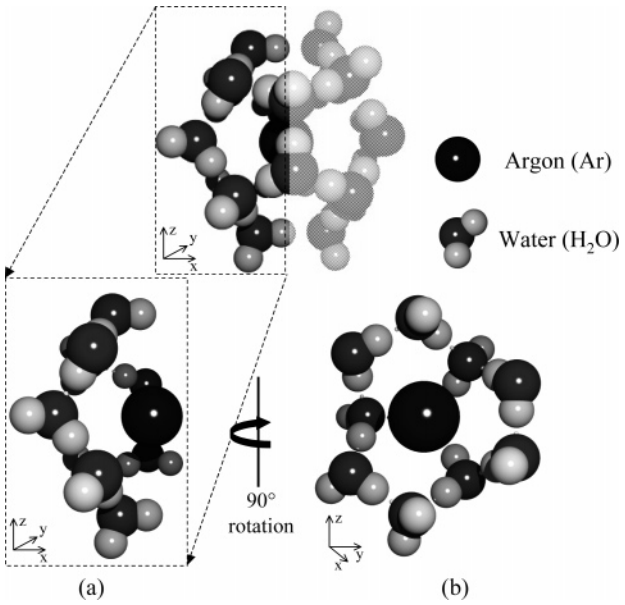


**Figure 6.** Two-dimensional projection of the half-cell configuration for argon in the small cage (pentagonal dodecahedron) of a structure II clathrate. (a) A $z-x$ planar orientation and (b) a $z-y$ planar orientation rotated 90° from (a) as shown. Relative atom sizes represent different $y$ in (a) and $x$ in (b) coordinate positions.

augmented basis sets) as we approach the size of the aug-cc-pVQZ basis set with 250 basis functions. The deviations of the binding energies, with respect to the aug-cc-pV5Z energy, are 0.015 and 0.006 kcal/mol for the aug-cc-pVTZ and aug-cc-pVQZ energies, respectively.

**Estimating Many-Body Effects.** The recent study by Klauda and Sandler[15] showed that many-body effects can result in a 35% change in the total energy of interaction between a clathrate cage and the guest molecule. To evaluate these effects in our study, a structure II pentagonal dodecahedron consisting of 20 water molecules surrounding entrapped argon and methane molecules (Figure 1a) was divided first into symmetrical halves then into quarters of a cell each containing 5 water molecules, as shown in Figure 6. Next the four cell quarters were each dissected into all of the combinations of two and three molecule combinations that could comprise each quarter cell. Finally, each set of two waters and three waters was split into its individual water molecules. The clathrate cage was then reconstructed piece by piece, calculating the energy to do so along the way. Interaction energies between the guest argon and each piece of the cage were calculated using MP2/aug-cc-ATZ ab initio methods and the developed **Ar**−**H**OH and $H_4$**C**−**H**OH potentials were corrected to reproduce the many-body cluster calculation.

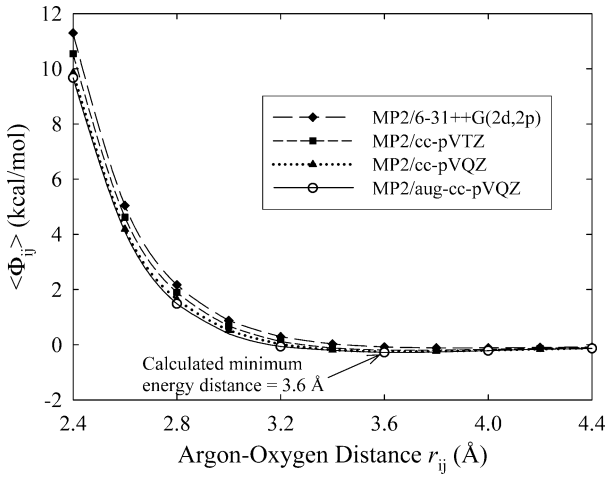


**Figure 7.** Effect of size of the basis set on the calculated ab initio pair potential for a binary Ar−$H_2O$ system.

**Reference Parameter Evaluation.** To determine reference parameters accurately for a structure II clathrate hydrate lattice, the approach by Holder et al.[27] was used. One can reformulate the temperature and pressure dependence of the multiphase equilibria criteria equating the chemical potential of water in hydrate (H) and liquid (L) or solid (α) phases, to give

$$Y = \frac{\Delta\mu_w^0}{RT_0} + \frac{\Delta H_w^0 + \Delta H_w^{\alpha-L}(T_0)}{R}\left[\frac{1}{T} - \frac{1}{T_0}\right] \qquad (8)$$

where $Y$ is a function of the experimental conditions ($T$, $P$, composition) and other properties, namely $\Delta b^{\beta-L \text{ or } \alpha}$, $\Delta C_p^{\beta-L \text{ or } \alpha}(T_0)$, and $\Delta V_w^{\beta-L \text{ or } \alpha}(T_0)$. In an earlier study,[30] we found accurate reference parameters for structure I clathrates using methane phase data and our calculated ab initio potential describing the methane−water interaction (see Table 1). A similar approach will be followed here to obtain reference parameters for structure II and structure I clathrates using the ab initio site−site potentials for argon and methane respectively in a water clathrate and accompanying phase data.

## Results and Discussion

**Basis Set Convergence.** Tsuzuki et al.[32] showed that a large basis set is needed to estimate accurately the interaction energy of hydrogen-bonded complexes. The basis set dependence of the binding energy of the Ar−$H_2O$ complex was evaluated. As a result, the MP2/aug-cc-pVQZ level and basis set were selected for the calculation of the ab initio potential energy surface between argon and water. Potential energy surfaces were determined using the MP2 level of electron correlation and the 6-31++G(2d,2p), cc-pVTZ, aug-cc-pVTZ, and aug-cc-pVQZ basis sets. These three-dimensional surfaces were then averaged and projected onto a spherically symmetric potential using the method described by Cao et al.[20] As shown in Figure 7, the potential converges as the size of the basis set approaches aug-cc-pVQZ.

The use of even larger basis sets was examined for the argon−water pair interaction. Table 2 shows the energy of the argon−water pair for the aug-cc-pVQZ and aug-cc-pV5Z basis sets. The difference in energies between the aug-cc-pVQZ and aug-cc-pV5Z basis sets shows that for this system convergence is reached to well within 0.14 kcal/mol, even for the short-range repulsive interaction at 2.4 Å. For distances of 2.8 Å or greater,

**TABLE 2: Comparison of aug-cc-pVQZ (AQZ) and aug-cc-pV5Z (A5Z) Calculations of the Angle-Averaged Binding Energy of an Ar−$H_2O$ Pair Using the MP2 Electron Correlation Level**

| $r$ (Å) | $\langle E_{cp,AQZ}(r)\rangle$ (kcal/mol) | $\langle E_{cp,A5Z}(r)\rangle$ (kcal/mol) |
|---|---|---|
| 2.4 | 9.365 | 9.233 |
| 2.8 | 1.097 | 1.059 |
| 3.2 | −0.294 | −0.305 |
| 3.6 | −0.347 | −0.352 |
| 4.0 | −0.230 | −0.232 |

[a] Energies reported in kcal/mol.

the difference in energy is lower, ranging from 0.04 to 0.002 kcal/mol, and lower than errors achieved by various basis set extrapolation methods.[33,34] This energy difference would not be visible if plotted in Figure 7.

The convergence of the ab initio potential was verified by examining the change in the thermodynamic properties resulting from the change in potential. For the argon−water system, convergence to within 0.01 kcal/mol in the attractive region of the potential was necessary to predict phase equilibria to within a 5% range.

**Grid Fineness.** Because accurate ab initio calculations are computationally intensive, it is desirable to optimize the grid spacing on the hyperspace ($r$, $\xi$, $\phi$, $\alpha$, $\beta$, $\gamma$) surface to achieve acceptable accuracy with the coarsest grid possible. Minimizing the total number of calculations necessary to achieve convergence of the potential increases efficiency substantially. By examining the sensitivity of the intermolecular potential we can evaluate the convergence of the potential for any grid size.

To ensure that a fine enough grid was used in the calculation of the final potential energy hypersurface at the MP2/aug-cc-pVQZ level, the effect of angular grid resolution was examined. Selected angular points were systematically removed from the Boltzmann averaging scheme to simulate a coarser mesh. As expected, there was a greater dependence of the potential on the $\xi$ grid points due to the interaction of the argon with the hydrogen atoms on the water molecule. Table 3 shows the results of systematically eliminating angular points on the average guest−host interaction energy.

Upon close inspection, one can see that the lower half of Table 3 illustrates the stronger dependence of the potential on the $\xi$ grid points. Elimination of grid points in the $\phi$ direction allows the potential to maintain its value to within 2%, whereas it diverges in a statistically significant manner from the converged curve when the grid in the $\xi$ direction is made coarser. Data for all 500 grid points per water plane, as discussed in Figure 3, are noted as all points. Elimination of angular grid points, ±20° and ±40°, in the $\xi$ and $\phi$ directions result in coarser meshes. The 20° spacing detailed earlier is sufficient to capture the effects of different orientations within the clathrate cage.

**Electron Correlation Effects.** Once convergence of the potential due to the grid size was achieved to ±3%, the level of electron correlation was examined. A size-consistent approach[35] was used to verify the convergence of the electron correlation energy using the aug-cc-pVQZ basis set, which was large enough to see convergence of the level of electron correlation.[36] As shown in Table 4, the calculated binding energies differ by less than 0.01 kcal/mol for the argon−water dimer at values of $r > 3$ Å between the MP2 and the MP4 level. This is in the attractive ($\Phi < 0$) region near the cell center. In the repulsive region, at smaller values of $r$, with argon closer to the cell boundaries, the errors are somewhat larger, but are proportionally weighted less due to the exponential Boltzmann factor in the configurational integral (see eq 2).

**Potential Forms.** Given a numerical argon−water pairwise ab initio potential, it is useful to have a mathematical form that can represent the calculated potential accurately. This would allow the potential to be easily implemented in the configurational integral for thermodynamic calculations or for molecular dynamics or Monte Carlo simulations. Figure 8 shows the least-squares fit of the angle-averaged ab initio potential to a few common two- and three-parameter potential forms, the Lennard-Jones 6-12, Kihara, and Exponential-6 potentials.

Lennard-Jones 6-12:

$$\Phi_{L-J}(r) = 4\epsilon\left[\left(\frac{\sigma}{r}\right)^{12} - \left(\frac{\sigma}{r}\right)^{6}\right] \quad (9)$$

Kihara:

$$\Phi_{Kihara}(r) = 4\epsilon\left[\left(\frac{\sigma - 2a}{r - 2a}\right)^{12} - \left(\frac{\sigma - 2a}{r - 2a}\right)^{6}\right] \quad (10)$$

Exponential-6:

$$\Phi_{Exp-6}(r) = \frac{\epsilon}{\alpha - 6}\left[6\exp\left(\alpha\left(1 - \frac{r}{r_m}\right)\right) - \left(\frac{r_m}{r}\right)^{6}\right] \quad (11)$$

Figure 8 clearly illustrates that the Exponential-6 and the Kihara potential forms provide the best description of the argon−water potential. The best fit for the Kihara potential, however, results in a nonphysical negative value for $a$ (−0.418 Å), the repulsive core diameter, so similarly to our previous work,[20] we conclude that the Exponential-6 potential[37] is the best for this interaction. Therefore, we used the exp-6 form to represent both the **Ar**−**O**$H_2$ and $H_4$**C**−**O**$H_2$ potentials. The Kihara potential form introduces a hard core repulsive effect that is inherently too strong to reproduce accurately the methane−water and argon−water interaction energies. The Kihara potential that best fits the ab initio data compensates for this softer core effect by introducing an aphysical attractive core radius ($a = -0.418$ Å). In a forthcoming paper[38] we report

**TABLE 3: Angle-Averaged Energy of Interaction of the Ar−$H_2O$ Pair at Different Radial Separation Distances for Varying Resolutions of Angular Grid Size**

| angles included in calculation (deg) | | total points per planar orientation | % deviation from full mesh | | | | |
|---|---|---|---|---|---|---|---|
| $\phi$ | $\xi$ | | $r = 2.4$ Å | $r = 2.8$ Å | $r = 3.2$ Å | $r = 3.6$ Å | $r = 4.0$ Å |
| −40, −20, 0, 20, 40 | −40, −20, 0, 20, 40 | 500 (all points) | 0.0 | 0.0 | 0.0 | 0.0 | 0.0 |
| −40, 0, 40 | −40, −20, 0, 20, 40 | 300 | 0.2 | −0.1 | 2.7 | 0.6 | 0.6 |
| −20, 0, 20 | −40, −20, 0, 20, 40 | 300 | −0.3 | −0.1 | −5.2 | −1.1 | −1.0 |
| 0 | −40, −20, 0, 20, 40 | 180 | −0.5 | −0.3 | −7.3 | −1.4 | −1.3 |
| −40, −20, 0, 20, 40 | −40, 0, 40 | 300 | 0.4 | −0.9 | −14.3 | 0.7 | 1.5 |
| −40, 0, 40 | −40, 0, 40 | 180 | 0.5 | −0.8 | −11.3 | 1.1 | 1.9 |
| −40, −20, 0, 20, 40 | −20, 0, 20 | 300 | −1.1 | −5.9 | 28.1 | −1.5 | −3.1 |
| −20, 0, 20 | −20, 0, 20 | 180 | −1.4 | −5.7 | 23.4 | −3.7 | −4.8 |
| −40, −20, 0, 20, 40 | 0 | 180 | −1.7 | −15.8 | 43.3 | −2.5 | −4.9 |
| 0 | 0 | 10 | −1.7 | −16.1 | 35.8 | −6.7 | −7.8 |

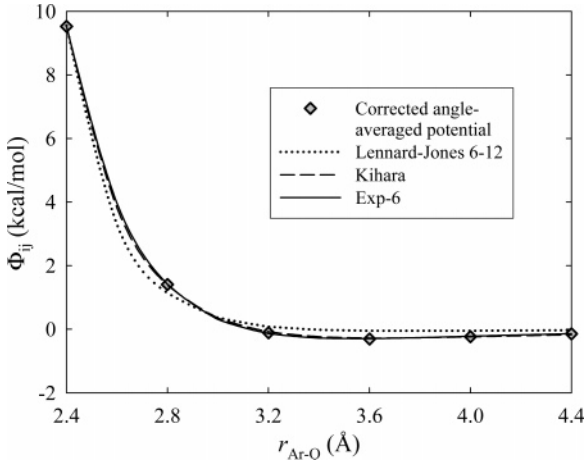


**Figure 8.** Selected potentials forms, Lennard-Jones 6-12, Kihara, and Exp-6, fitted to the ab initio calculated Ar−$H_2O$ intermolecular potential.

**TABLE 4: Comparison of MP2 and MP4 Calculations of the Angle-Averaged Binding Energy of an Ar−$H_2O$ Pair Using the aug-cc-pVQZ Basis Set**

| $r$ (Å) | $\langle E_{cp,MP2}(r)\rangle$ (kcal/mol) | $\langle E_{cp,MP4}(r)\rangle$ (kcal/mol) |
|---|---|---|
| 2.4 | 9.365 | 9.489 |
| 2.8 | 1.097 | 1.109 |
| 3.2 | −0.294 | −0.301 |
| 3.6 | −0.347 | −0.352 |
| 4.0 | −0.230 | −0.232 |

that the Kihara potential can reproduce accurately the methane Langmuir constants for structure I hydrates, but not for structure II, a direct result of this phenomenon. The "hardness" of the Kihara potential for the methane−water interaction in a structure II lattice causes the fitted reference chemical potential[8] to be significantly lower than the value measured by experiment. Further potential parameter adjustment is necessary when modeling systems involving structure I to structure II phase transitions,[39] emphasizing the current "ad hoc" nature of modeling using such aphysical potential models.

The **Ar**−**H**OH and $H_4$**C**−**H**OH interactions were characterized by a purely repulsive interaction and were modeled using

$$\Phi_{repul}(r) = \frac{B}{r^{12}} \tag{12}$$

and the $H_3$C**H**−**O**$H_2$ interaction was modeled using the L-J 6-12 potential. The 500 argon−water ab initio energies and the 18 000 methane−water ab initio energies were fit to the site−site potentials minimizing $\chi$ in the following objective function:[15]

$$\chi = \sum_{i}^{\text{no. of QM points}} \left[ \exp\left(\frac{-\Delta E_{cp,i}}{kT}\right)_{pred} - \exp\left(\frac{-\Delta E_{cp,i}}{kT}\right)_{QM} \right]^2 \tag{13}$$

The temperature, $T$, used in eq 13 was 273 K; however, our sensitivity analysis shows that within the range of temperatures 150−300 K, the choice of $T$ results in deviations of optimum potential parameters of less than 4%. The adjustable parameters in the site−site potentials are the characteristic energy, $\epsilon$, for both the L-J 6-12 and the exp-6 potentials, the soft core radius, $\sigma$, of the L-J 6-12 potential, the radius of minimum energy, $r_m$, of the exp-6 potential, and $B$ for the repulsive interactions. The $\alpha$ values of the exp-6 potentials were held constant at 12.5 Å for argon and 12.15 Å for methane.

**Many-Body Effects.** Many-body interaction effects were also evaluated. In principle, we are interested in estimating the total potential energy for all water molecules in the full cage interacting with a single argon molecule. Due to computational limitations we were only able to calculate many body effects using 10 water molecules in half of the pentagonal dodecahedron−cell A (Figure 1a) with a single guest argon at the MP2/aug-cc-pVQZ level. Klauda and Sandler[15] showed at a lower level of accuracy for the $CH_4$−$H_2O$ system that two half-cell calculations closely resemble the calculation of the full cell. Therefore, we assumed a similar trend would hold for the argon−water system and evaluated a number of partial-cell structures to analyze the many-body effect. Table 5 shows the calculation of the total interaction energy between an argon guest and a structure II pentagonal dodecahedron using various sums of pair and many-body interactions. The quarter cell calculated energies have converged to within 0.04 kcal/mol of the half cell energy and thus will be used in subsequent many-body calculations. The guest molecule was then placed in a number of different configurations within the quarter cell, and the interaction energy was calculated for this 6-molecule system.

**TABLE 5: Calculation of Interaction Energy between the Entrapped Argon Guest Located at the Cell Center and Full Pentagonal Dodecahedron Cell with 20 Host Water Molecules Using Half and Quarter Cells, and Sums of Pieces of Quarter Cells (Groups of 2 and 3 Waters)**

| method of ab initio calculation | interaction energy (kcal/mol) |
|---|---|
| half cell (10 waters) × 2 | −4.338 |
| quarter cell (5 waters) × 4 | −4.371 |
| assembled groups of 2 and 3 waters (20 total) | −4.083 |

[a] Note that only the first shell Ar−$H_2O$ interactions are included.

**TABLE 6: Fit Potential Parameters for the ab Initio Site−Site Models for Ar−$H_2O$**

| | Exponential-6 | | | repulsive |
|---|---|---|---|---|
| interaction | $\epsilon/k$ (K) | $r_m$ (Å) | $\alpha$ | $B$ (Å$^{12}$ kcal/mol) |
| **Ar**−**O**$H_2$ | 156.8 | 3.556 | 12.5 | |
| **Ar**−**H**OH | | | | $1.259 \times 10^5$ |

The site−site model was then used to calculate the total interaction energy of the many-body system. The water−water interactions within the hydrate lattice are primarily along the cage vertexes, and the resulting delocalization of electrons along the hydrogen bond will serve to affect the strength of the guest−hydrogen interaction. Consequently, to account for this hydrogen bond effect in the argon−water system, the pairwise ab initio site−site potential was corrected by adjusting the characteristic energy, $\epsilon_{Ar-H}$, of the **Ar**−**H**OH L-J potential such that the errors of the predictions of the site−site model with respect to the ab initio quarter cage calculations were minimized. The optimized site−site potential parameters for argon and methane with water are listed in Table 6. The results of the predictions of the quarter cell−argon interaction energies using the uncorrected and corrected site−site potentials are shown in Figure 9. Similarly, the methane ab initio site−site potential was used to predict the quarter cell−methane interaction energy; however, no correction was needed to represent properly the many-body system. The results of the methane 6-molecule system predicted energies are shown in Figure 10.

One can see from Figure 10 that the methane site−site potential reproduces the interaction energies of the many body system with high accuracy without any correction to the $H_4$**C**−**H**OH potential. Any correction attempt results in a negligible change to $\epsilon_{C-H}$. The argon−water interaction is principally dispersive in nature and is much more sensitive to changes in the water electron structure than the methane−water interaction.

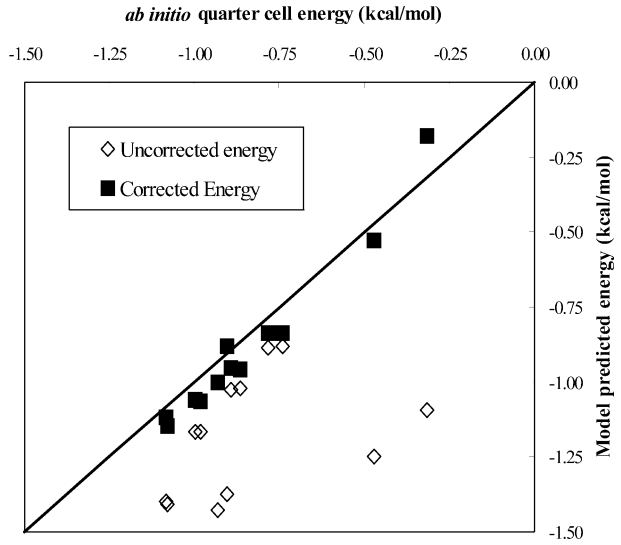


**Figure 9.** Parity plot of the uncorrected and corrected site−site predicted quarter cell−argon interaction energy.

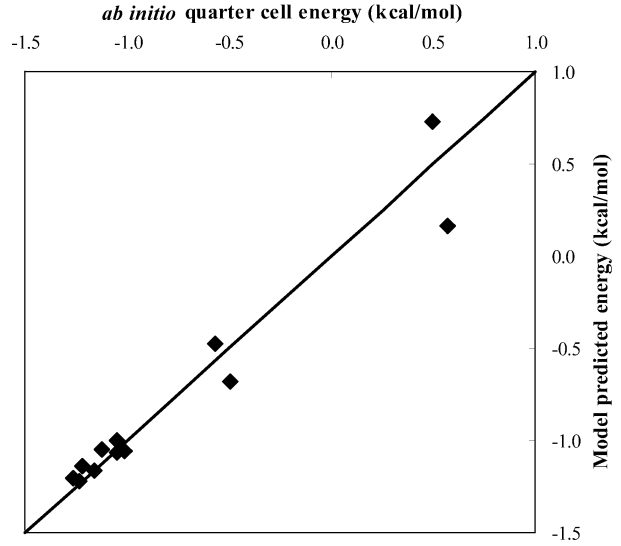


**Figure 10.** Parity plot of the uncorrected site−site predicted quarter cell−methane interaction energies.

**Determination of Reference Parameters.** Using the method first developed by Holder et al.[27] and the ab initio pair potential for Ar−$H_2O$ interactions, we determined the references parameters for a structure II hydrate lattice to be $\Delta\mu_w^0 = 1077 \pm 5$ J/mol and $\Delta H_w^0 = 1297 \pm 11$ J/mol (see Figure 11). The estimation of the error in the calculation of the reference parameters was found by calculating the 95% confidence intervals on the regression; it slightly underestimates the overall error because experimental errors were not included. The choice of $\chi$ in eq 13 will affect the calculated reference parameters; however, over the range of experimental temperatures, the deviations in $\Delta\mu_w^0$ and $\Delta H_w^0$ that result ($\pm 4$ and $\pm 9$ J/mol, respectively) are within the 95% confidence intervals. The reference parameter results compare favorably with the structure II reference parameters found by Handa and Tse[40] using thermophysical data from the krypton structure II hydrate. We have also used our method for calculating reference parameters in conjunction with the argon potential found by Tee et al.[41] using second virial coefficients and viscosity data and the potential found by Bickes et al.[42] via molecular-beam differential scattering measurements on argon with water. These results are tabulated in Table 8.

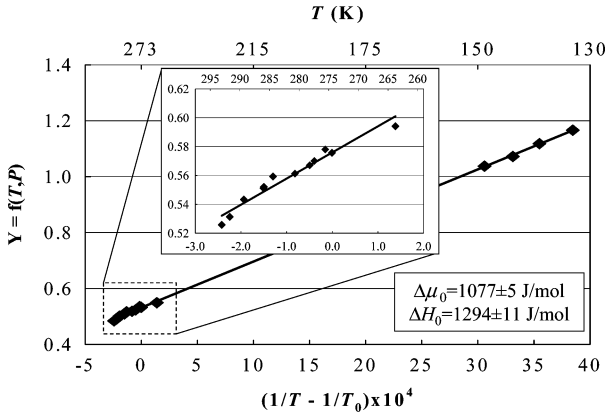


**Figure 11.** Determination of structure II reference parameters using the Holder et al.[27] method, $Y = f(T,P)$ from eq 8, and experimental data from Barrer and Edge[43] and Saito and Kobayashi.[44]

**TABLE 7: Fit Potential Parameters for the ab Initio Site−Site Models for $CH_4$−$H_2O$**

| | Exponential-6 | | | repulsive | L-J 6-12 | |
|---|---|---|---|---|---|---|
| interaction | $\epsilon/k$ (K) | $r_m$ (Å) | α | $B$ (Å$^{12}$ kcal/mol) | $\epsilon/k$ (K) | $\sigma$ (Å) |
| $H_4C-OH_2$ | 165.1 | 3.634 | 10.15 | | | |
| $H_4C-HOH$ | | | | $2.792 \times 10^5$ | | |
| $H_3CH-OH_2$ | | | | | 16.7 | 2.03 |

This process was repeated for structure I using the calculated ab initio site−site potential for methane and water and the reference parameters were determined to be be $\Delta\mu_w^0 = 1203 \pm 3$ J/mol and $\Delta H_w^0 = 1170 \pm 19$ J/mol. These results, along with the above structure II results are listed in Table 1.

**Phase Equilibrium Calculations.** Using the regressed reference parameters given in Figure 11 and Table 8 for a structure II hydrate, we are now able to reproduce experimental equilibrium data for the argon−water clathrate. Figures 12 and 13 demonstrate the robustness of the method employed in this paper. The model agrees with experimental results to ±3% over a wide temperature (133−293 K) and pressure range (0.3−850 bar). The reference parameters listed in Table 8 were used for phase equilibria calculations plotted in Figure 13 for the three different Ar−$H_2O$ potentials.

The methane−water site−site potential in conjunction with the calculated structure I reference parameters leads to a 3.5% absolute average deviation (AAD) from experimental data. This match is achieved with only two adjustable parameters, $\Delta\mu_w^0$ and $\Delta H_w^0$, which we will show in a forthcoming paper on hydrate cell potentials to be applicable to not only the methane hydrate system but for other structure I hydrate formers.[38] Using the LJD approximation and Sloan's[8] Kihara parameters, the AAD is 11% and Klauda and Sandler[15] report an AAD of 3.35% for structure I methane hydrates. The Klauda and Sandler[15] method uses three parameters to fit the pure data, whereas we achieve 3.5% AAD using two parameters that are applicable to other hydrate systems. The Klauda and Sandler methane potentials are dependent on the cage and the values for $\epsilon$ in the L-J 6-12 potential vary by as much as 15% with the chosen cage. Our methane and argon potentials are independent of structure and location and should be applicable to any condensed aqueous system.

**Methane Cage Occupancies.** Cage occupancies have been measured using Raman spectroscopy and nuclear magnetic resonance (NMR) techniques.[45−47] These techniques rely on the integration of signal intensities characteristic of guests occupying different cages. The ratios of the integrated intensities reproduce the ratios of the occupancies of the guest in the lattice cages,

**TABLE 8: Theoretical Empty Hydrate Reference Parameters for Structure II Hydrates**

| method of Ar−$H_2O$ interaction | $\Delta\mu_w^0$ (J/mol) | $\Delta H_w^0$ (J/mol) | sources |
|---|---|---|---|
| 2nd virial/viscosity Kihara | 1073 | 1900 | Tee et al.[41] |
| molecular-beam scattering L-J 6-12 | 1180 | 920 | Bickes et al.[42] |
| thermophysical properties of krypton sII | 1068 | 764 | Handa & Tse[40] |
| ab initio interaction with many-body correction | 1077 | 1294 | This study |

scaled by the ratio of the total number of cages in a unit cell. Ripmeester and Ratcliffe[45] used NMR to study the occupancy ratios of methane and methane−propane hydrates. The pure methane hydrate occupancy ratio, $\theta_S/\theta_L$ was measured to be 0.916, where $\theta_L$ and $\theta_S$ are large- and small-cage occupancies, respectively. The hydrate samples were conditioned for ∼3 months at 233 K and then for ∼1 week at 260 K. They were then cooled to 77 K and placed into the NMR probe that had been cooled to ∼193 K. Using this procedure, the hydrate should exhibit properties of a hydrate conditioned at 260 K, and this is the temperature that was used by Ripmeester and Ratcliffe to calculate the absolute occupancies. We used the Klauda and Sandler[15] method to calculate $\theta_S/\theta_L(193\text{ K}) = 0.84$ as they did and then using their potential results in $\theta_S/\theta_L(260\text{ K}) = 0.84$.

Uchida et al.[47] measured methane hydrate occupancy using Raman spectroscopy at pressures above the equilibrium pressure.

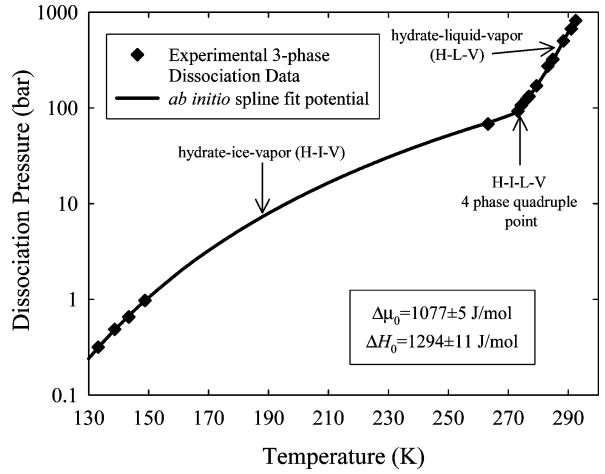


**Figure 12.** Calculation of argon three-phase equilibrium dissociation pressures using the corrected ab initio site−site potential with the regressed structure II reference parameters. Experimental data are from Barrer and Edge[43] and Saito and Kobayashi.[44]

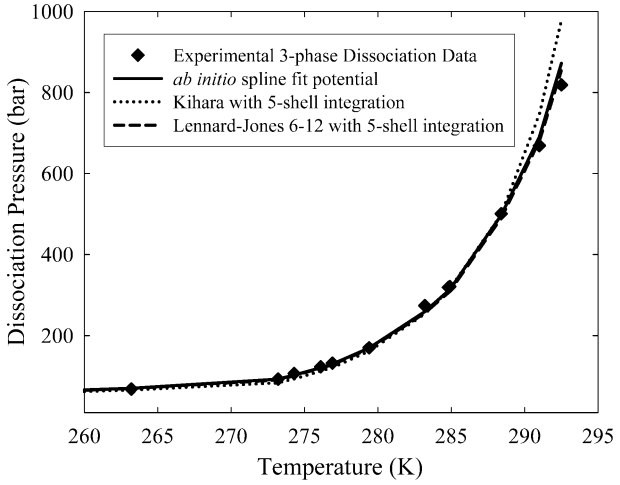


**Figure 13.** Comparison of experimental three-phase equilibrium dissociation pressures[43,44] for the argon hydrate system with predictions using the ab initio potential developed in this study, the Kihara potential found by Tee et al.[41] and the L-J 6-12 parameters found by Bickes et al.[42]

**TABLE 9: Occupancy Ratio, $\theta_S/\theta_L$, of Methane Structure I Hydrates**[a]

| temp (K) | exp value[45,46] | CSMHYD[8] | this study |
|---|---|---|---|
| 260 | 0.916 ± 0.01 | 0.910 | 0.920 |
| 273.65 | 0.947 ± 0.02 | 0.900 | 0.906 |
| 274.65 | 0.925 ± 0.02 | 0.904 | 0.910 |
| 275.65 | 0.892 ± 0.03 | 0.908 | 0.914 |
| 276.65 | 0.890 ± 0.01 | 0.912 | 0.917 |

[a] CSMHYD indicates the phase equilibria program included in Sloan, 1998.[8]

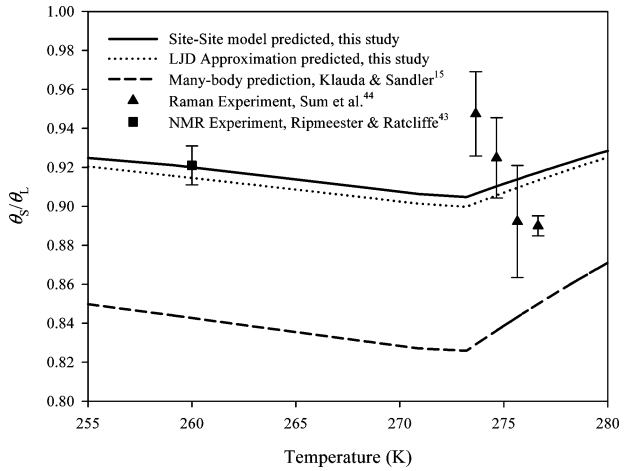


**Figure 14.** Temperature dependence of the ocupancy ratio $\theta_S/\theta_L$ of methane structure I hydrates.

However, the specific pressure at which the samples were conditioned cannot be determined from their paper. The reaction vessel was pressurized to the specific pressure then as the hydrate formed the pressure dropped. The final pressure is the pressure of importance, though the "specific" pressure is reported. Moreover, with increasing pressure they report a decreasing $\theta_S/\theta_L$, which is contrary to expectations. Sum et al. also used Raman spectroscopy to measure methane cage occupancies at the equilibrium pressure.[46] Using our methane ab initio site−site model, we calculate the occupancy ratios reported by the Ripmeester[45] and Sum[46] groups, as detailed in Table 9.

**Mixed Hydrate Phase Equilibrium.** Because argon preferentially forms a structure II hydrate and methane preferentially forms a structure I hydrate, there should be a surface in the argon−methane−water phase diagram where a structural change would occur. We can calculate and predict where this structural change would occur. The ability of our model to predict phase equilibria in the mixed argon−methane hydrate provides an independent test of our intermolecular potentials and calculated reference parameters of the two hydrate structures, as shown in Figure 15. Figure 15 also illustrates where the structural transition is predicted on the basis of thermodynamic equilibrium.

Within the experimental temperature range, the structure I to structure II transition occurs near 0.4 mol fraction methane. Because the difference in free energy of the two structures near 40% methane is very small, a particular solid hydrate phase once formed could remain in a metastable state even after

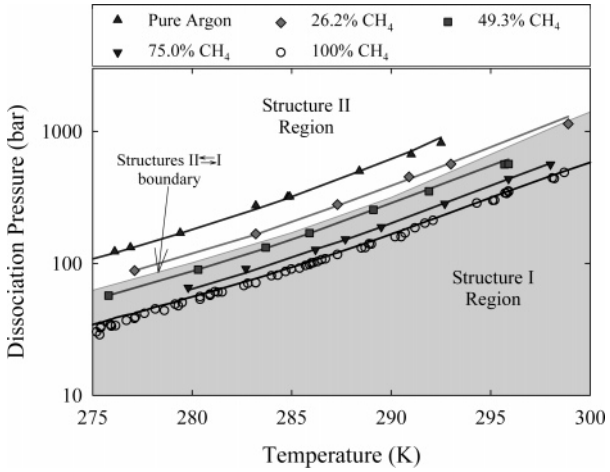


**Figure 15.** Predicted dissociation pressure of mixed $CH_4-Ar$ hydrate using the calculated ab initio potential for both guest species. Experimental data are given for pure Ar (▲), 26.2% $CH_4$ (◆), 49.3% $CH_4$ (■), 75% $CH_4$ (▼), 100% $CH_4$ (○). Predictions (—) are calculated using the lowest energy structure.

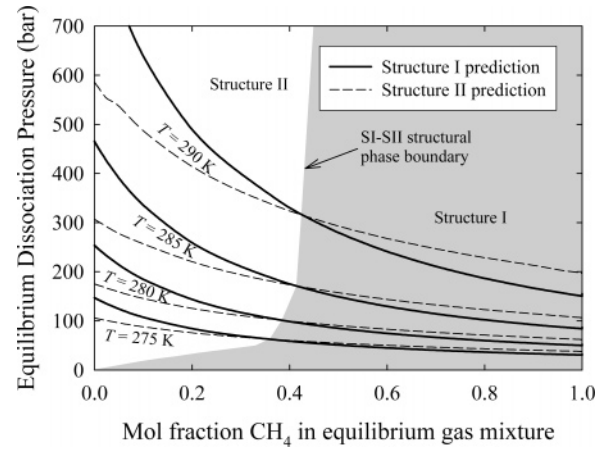


**Figure 16.** Prediction of structural changes in a mixed $Ar-CH_4$ hydrate at 275, 280, 285, and 290 K. Solid lines are structure I and dotted lines are structure II predicted dissociation pressures for the three-phase (hydrate—water-rich liquid—gas mixture) monovariant systems.

entering the stable region for the other structure. In other words, if one were to add argon gas to a system in which a structure I hydrate had already been formed with methane as a guest gas, it could continue to crystallize as a structure I hydrate. In general, the structure that would result from nucleating a mixture of argon and methane could be governed by kinetics. Figure 16 demonstrates the ability of this model to predict the structural transition that is likely to exist when the composition of an argon—methane gas mixture is changed.

## Conclusions

Accurate quantum mechanical calculations were performed to quantify argon—water interactions for use in modeling the condensed gas hydrate system. Convergence to within 0.01 kcal/mol in the attractive region was reached for the argon—water binary system at the MP2/aug-cc-pVQZ level of correlation and basis-set. A site—site potential was developed that characterizes the three-dimensional hyperspace energy surface of the argon—water interaction and the six-dimensional surface for methane—water interactions. Many-body effects can be significant in the argon—water system due to the delocalization of electrons along the hydrogen bonds. These effects were accounted for by fitting the **Ar**—**H**OH potential characteristic energy to quantum mechanical calculations on systems with up to five water molecules interacting with the argon. The many-body effects are negligible in the methane—water system when our methane—water site—site potential is used. Precise values for structure II reference parameters, $\Delta\mu_w^0 = 1077 \pm 5$ kcal/mol and $\Delta H_w^0 = 1294 \pm 11$ kcal/mol and structure I reference parameters, $\Delta\mu_w^0 = 1203 \pm 3$ kcal/mol and $\Delta H_w^0 = 1170 \pm 19$ kcal/mol (errors evaluated using 95% confidence intervals), were found using the ab initio site—site potentials. Using these reference values together with the ab initio site—site potentials, the equilibrium dissociation pressure was computed within ±3% of the experimental value for pure argon hydrates and within ±3.5% of the experimental value for methane hydrates. Over the temperature range studied, we verified that argon forms structure II hydrates as opposed to structure I hydrates. Methane cage occupancies were predicted to within ±5% of experimental values. Phase equilibria for the mixed hydrate of argon and methane were predicted within ±3.4% without any fitting parameters. Also the existence of structure I to structure II phase transitions was determined using our ab initio approach.

**Acknowledgment.** We thank the Singapore-MIT Alliance and the Martin Foundation for its partial support of this research. We also gratefully acknowledge Prof. William Green, Prof. John Deutch, and Dr. Zhitao Cao for their insightful contributions to this work. We also acknowledge the other members of our research groups at MIT and Dr. Kevin Sparks for their help and support.

## References and Notes

(1) Davidson, D. W.; Garg, S. K.; Gough, S. R.; Handa, Y. P.; Ratcliffe, C. I.; Ripmeester, J. A. *J. Inclusion Phenomena* **1984**, *2*, 231.
(2) Tse, J. S.; Handa, Y. P.; Ratcliffe, C. I.; Powell, B. M. *J. Inclusion Phenomena* **1986**, *4*, 235.
(3) van der Waals, J. H.; Platteeuw, J. C. *Adv. Chem. Phys.* **1959**, *2*, 1.
(4) Peng, D.-Y.; Robinson, D. B. *Ind. Eng. Chem. Fundam.* **1976**, *15*, 59.
(5) Sparks, K. A.; Tester, J. W. *J. Phys. Chem.* **1992**, *96*, 11022.
(6) Sparks, K. A.; Tester, J. W.; Cao, Z. T.; Trout, B. L. *J. Phys. Chem. B* **1999**, *103*, 6300.
(7) Holder, G. D.; John, V. T.; Yen, S. Geological implications of gas production from In-situ gas hydrates. SPE/DOE symposium on unconventional gas recovery, 1980.
(8) Sloan, E. D., Jr. *Clathrate hydrates of natural gases*, 2nd ed., rev. and expanded; Marcel Dekker: Monticello, 1998.
(9) Hammerschmidt, E. G. *Ind. Eng. Chem.* **1934**, *26*, 851.
(10) Fowler, R. H.; Guggenheim, E. A. *Statistical Thermodynamics*; Cambridge University Press: Cambridge, U.K., 1952.
(11) John, V. T.; Papadopoulos, K. D.; Holder, G. D. *AIChE J.* **1985**, *31*, 252.
(12) Sparks, K. A. Configurational properties of water clathrates through molecular simulation, Ph.D. Thesis, Massachusetts Institute of Technology, 1991.
(13) Bazant, M. Z.; Trout, B. L. *Physica A* **2001**, *300*, 139.
(14) John, V. T.; Holder, G. D. *J. Phys. Chem.* **1985**, *89*, 3279.
(15) Klauda, J. B.; Sandler, S. I. *J. Phys. Chem. B* **2002**, *106*, 5722.
(16) Cao, Z.; Tester, J. W.; Trout, B. L. *J. Chem. Phys.* **2001**, *115*, 2550.
(17) Jorgensen, W. L.; Madura, J. D.; Swenson, C. J. *J. Am. Chem. Soc.* **1984**, *106*, 6638.
(18) Sun, Y.; Kollman, P. A. *J. Comput. Chem.* **1995**, *16*, 1164.
(19) Cao, Z. T.; Tester, J. W.; Sparks, K. A.; Trout, B. L. *J. Phys. Chem. B* **2001**, *105*, 10950.
(20) Cao, Z. T.; Tester, J. W.; Trout, B. L. *J. Chem. Phys.* **2001**, *115*, 2550.
(21) Barrer, R. M.; Ruzicka, D. J. *Trans. Faraday Soc.* **1962**, *58*, 2253.
(22) Sortland, L. D.; Robinson, D. B. *Can. J. Chem. Eng.* **1964**, *42*, 38.
(23) Child, W. C., Jr. *J. Phys. Chem.* **1964**, *68*, 1834.
(24) Parrish, W. R.; Prausnitz, J. M. *Ind. Eng. Chem. Process Des. Dev.* **1972**, *11*, 26.
(25) Holder, G. D.; Katz, D. L.; Hand, J. H. *AAPG Bull.-Am. Association of Petroleum Geol.* **1976**, *60*, 981.

(26) Dharmawardhana, P. B.; Parrish, W. R.; Sloan, E. D. *Ind. Eng. Chem. Fundam.* **1980**, *19*, 410.
(27) Holder, G. D.; Malekar, S. T.; Sloan, E. D. *Ind. Eng. Chem. Fundam.* **1984**, *23*, 123.
(28) Davidson, D. W.; Handa, Y. P.; Ripmeester, J. A. *J. Phys. Chem.* **1986**, *90*, 6549.
(29) Handa, P. Y.; Tse, J. S. *J. Phys. Chem.* **1986**, *90*, 5917.
(30) Cao, Z. T.; Tester, J. W.; Trout, B. L. *J. Phys. Chem. B* **2002**, *106*, 7681.
(31) Dunning, T. H. *J. Phys. Chem. A* **2000**, *104*, 9062.
(32) Tsuzuki, S.; Uchimaru, T.; Matsumura, K.; Mikami, M.; Tanabe, K. *J. Chem. Phys.* **1999**, *110*, 11906.
(33) Truhlar, D. G. *Chem. Phys. Lett.* **1998**, *294*, 45.
(34) Varandas, A. J. C. *J. Chemi. Phys.* **2000**, *113*, 8880.
(35) Chakravorty, S. J.; Davidson, E. R. *J. Phys. Chem.* **1993**, *97*, 6373.
(36) Feller, D. *J. Chem. Phys.* **1999**, *111*, 4373.
(37) Ree, F. H. *Simple molecular systems at very high density*; Plenum: New York, 1989.
(38) Anderson, B. J.; Bazant, M. Z.; Tester, J. W.; Trout, B. L. *J. Phys. Chem. B*, submitted.
(39) Ballard, A. L.; Sloan, E. D. *Gas Hydrates: Challenges for the Future* **2000**, *912*, 702.
(40) Handa, Y. P.; Tse, J. S. *J. Phys. Chem.* **1986**, *90*, 5917.
(41) Tee, L. S.; Gotoh, S.; Stewart, W. E. *Ind. Eng. Chem. Fundam.***1966**, *5*, 363.
(42) Bickes, R. W.; Scoles, G.; Smith, K. M. *Can. J. Phys.* **1975**, *53*, 435.
(43) Barrer, R. M.; Edge, A. V. J. *Proc. R. Soc., London* **1967**, *A300*, 1.
(44) Saito, S.; Kobayashi, R. *AIChE J.* **1965**, *11*, 96.
(45) Ripmeester, J. A.; Ratcliffe, C. I. *J. Phys. Chem.* **1988**, *92*, 337.
(46) Sum, A. K.; Burruss, R. C.; Sloan, E. D. *J. Phys. Chem. B* **1997**, *101*, 7371.
(47) Uchida, T.; Hirano, T.; Ebinuma, T.; Narita, H.; Gohara, K.; Mae, S.; Matsumoto, R. *AIChE J.* **1999**, *45*, 2641.